

1-7-2023

Mst1-Mediated Phosphorylation of Nur77 Improves the Endometrial Receptivity in Human and Mice

Xinyu Cai

Yue Jiang

Zhiwen Cao

Mei Zhang

Na Kong

See next page for additional authors

Follow this and additional works at: <https://jdc.jefferson.edu/transmedfp>



Part of the [Translational Medical Research Commons](#)

[Let us know how access to this document benefits you](#)

This Article is brought to you for free and open access by the Jefferson Digital Commons. The Jefferson Digital Commons is a service of Thomas Jefferson University's [Center for Teaching and Learning \(CTL\)](#). The Commons is a showcase for Jefferson books and journals, peer-reviewed scholarly publications, unique historical collections from the University archives, and teaching tools. The Jefferson Digital Commons allows researchers and interested readers anywhere in the world to learn about and keep up to date with Jefferson scholarship. This article has been accepted for inclusion in Center for Translational Medicine Faculty Papers by an authorized administrator of the Jefferson Digital Commons. For more information, please contact: JeffersonDigitalCommons@jefferson.edu.

Authors

Xinyu Cai, Yue Jiang, Zhiwen Cao, Mei Zhang, Na Kong, Lina Yu, Yedong Tang, Shuangbo Kong, Wenbo Deng, Haibin Wang, Jianxin Sun, Lijun Ding, Ruiwei Jiang, Haixiang Sun, and Guijun Yan

Mst1-mediated phosphorylation of Nur77 improves the endometrial receptivity in human and mice

Xinyu Cai,^{a,b,g} Yue Jiang,^{a,b,g} Zhiwen Cao,^{a,b,g} Mei Zhang,^{a,b} Na Kong,^{a,b} Lina Yu,^{a,b} Yedong Tang,^c Shuangbo Kong,^c Wenbo Deng,^c Haibin Wang,^c Jianxin Sun,^d Lijun Ding,^{a,b} Ruiwei Jiang,^{a,b,*} Haixiang Sun,^{a,b,e,**} and Guijun Yan^{a,b,f,***}

^aCenter for Reproductive Medicine and Obstetrics and Gynecology, Nanjing Drum Tower Hospital, Nanjing University Medical School, Nanjing, China

^bCenter for Molecular Reproductive Medicine, Nanjing University, Nanjing, China

^cReproductive Medical Center, The First Affiliated Hospital of Xiamen University, Xiamen, PR China

^dDepartment of Medicine, Center for Translational Medicine, Thomas Jefferson University, Philadelphia, PA, 19107, USA

^eState Key Laboratory of Reproductive Medicine, Nanjing Medical University, Nanjing, China

^fState Key Laboratory of Pharmaceutical Biotechnology, Nanjing University, 210032 Nanjing, China

Summary

Background Successful embryo implantation requires the attachment of a blastocyst to the receptive endometrial epithelium, which was disturbed in the women with recurrent implantation failure (RIF). Endometrial β 3-integrin was the most important adhesion molecule contributing to endometrial receptivity in both humans and mice. Nur77 has been proven indispensable for fertility in mice, here we explore the role of Nur77 on embryo-epithelial adhesion and potential treatment to embryo implantation failure.

Methods The expression and location of Mst1 and Nur77 in endometrium from fertile women and RIF patients were examined by IHC, qRT-PCR and Western blotting. In vitro kinase assay following with LC-MS/MS were used to identify the phosphorylation site of Nur77 activated by Mst1. The phosphorylated Nur77 was detected by phos-tag SDS-PAGE assay and specific antibody against phospho-Nur77-Thr366. The effect of embryo-epithelium interaction was determined in the BeWo spheroid or mouse embryo adhesion assay, and delayed implantation mouse model. RNA-seq was used to explore the mechanism by which Nur77 derived peptide promotes endometrial receptivity.

Findings Endometrial Mammalian sterile 20 (STE20)-like kinase 1 (Mst1) expression level was decreased in the women with RIF than that in the fertile control group, while Mst1 activation in the epithelial cells promoted trophoblast–uterine epithelium adhesion. The effect of Nur77 mediated trophoblast–uterine epithelium adhesion was facilitated by active Mst1. Mechanistically, mst1 promotes the transcription activity of Nur77 by phosphorylating Nur77 at threonine 366 (T366), and consequently increased downstream target β 3-integrin expression. Furthermore, a Nur77-derived peptide containing phosphorylated T366 markedly promoted mouse embryo attachment to Ishikawa cells ([4 (2–4)] vs [3 (2–4)]) and increased the embryo implantation rate (4 vs 1.4) in a delayed implantation mouse model by regulating integrin signalling. Finally, it is observed that the endometrial phospho-Nur77 (T366) level is decreased by 80% in the women with RIF.

Interpretation In addition to uncovering a potential regulatory mechanism of Mst1/Nur77/ β 3-integrin signal axis involved in the regulation of embryo-epithelium interaction, our finding provides a novel marker of endometrial receptivity and a potential therapeutic agent for embryo implantation failure.

Funding National Key Research and Development Program of China (2018YFC1004400), the National Natural Science Foundation of China (82171653, 82271698, 82030040, 81971387 and 30900727), and National Institutes of Health grants (R01HL103869).

*Corresponding author. Reproductive Medicine Center, The Affiliated Drum Tower Hospital of Nanjing University Medical School, Nanjing, 210008, PR China.

**Corresponding author. Reproductive Medicine Center, The Affiliated Drum Tower Hospital of Nanjing University Medical School, Nanjing, 210008, PR China.

***Corresponding author. Reproductive Medicine Center, The Affiliated Drum Tower Hospital of Nanjing University Medical School, Nanjing, 210008, PR China.

E-mail addresses: rwjiang@smail.nju.edu.cn (R. Jiang), haixiang_sun@nju.edu.cn (H. Sun), yanguijun@nju.edu.cn (G. Yan).

[§]These authors contributed equally to this work.



eBioMedicine
2023;88: 104433
Published Online xxx
<https://doi.org/10.1016/j.ebiom.2022.104433>

Copyright © 2022 The Author(s). Published by Elsevier B.V. This is an open access article under the CC BY-NC-ND license (<http://creativecommons.org/licenses/by-nc-nd/4.0/>).

Keywords: Embryo implantation; Mst1; Nur77; Peptide; β 3-integrin

Research in context

Evidence before this study

Inadequate endometrial receptivity is responsible for approximately two-thirds of implantation failures. Adhesion molecules have been proven to be involved in the attachment of blastocyst to uterine epithelium. Previous studies have demonstrated that the β 3-integrin plays an important role in the establishment of endometrial receptivity in human and mice. A Nur77-derived peptide has been shown to induce the apoptosis of cancer cells *in vitro* and in animals. We previously reported that Nur77 knockout mice exhibited impaired decidualization and a subfertility phenotype. However, it is not clear about the molecular function of Nur77 and the potential regulatory relationship between Nur77 and β 3-integrin in the establishment of endometrial receptivity.

Added value of this study

We found that Mst1 is involved in establishing endometrial receptivity dependent on the kinase activity, and identified Nur77 as a new substrate of Mst1. Mst1 phosphorylates Nur77 at threonine 366 to regulate the transcription of

β 3-integrin. Importantly, we uncovered that peptide-pThr³⁶⁶ promoted trophoblast-uterine epithelium adhesion *in vitro* and embryo implantation *in vivo* and endometrial pNur77 (T366) level was aberrantly decreased in women with RIF, indicating the key role of Mst1 mediated phosphorylation of Nur77 on endometrial receptivity.

Implications of all the available evidence

This study uncovered a potential regulatory mechanism of Mst1/Nur77/ β 3-integrin signal axis involved in the establishment of endometrial receptivity in human and mice. We demonstrated that a Nur77-derived peptide-pThr³⁶⁶ promoted the embryo-epithelium interaction, and endometrial phospho-Nur77 (T366) was a promising biomarker for endometrial receptivity. A better understanding of the regulatory network of the Mst1/Nur77/ β 3-integrin signal axis may help to develop related targeted therapy for clinical treatment of recurrent embryo implantation failure in women.

Introduction

Successful implantation of embryos into the maternal uterine endometrium is a crucial step in mammalian reproduction. In humans, natural conception during one menstrual cycle is not higher than 30%.¹ Embryo implantation failure contributes to 70% of all pregnancy losses and are responsible for the relative inefficiency of embryo transfer in infertile couples undergoing assisted reproductive technologies (ART).^{2,3} It was estimated that there is a 90% of cumulative pregnancy rate after the transfer of at least four blastocysts.⁴ Absence of a clinical pregnancy after the indicated attempts is considered an acceptable definition for recurrent implantation failure (RIF), in which inadequate endometrial receptivity plays a key factor.^{5,6} The uterus is receptive to blastocyst implantation during a restricted time period termed “window of implantation”, 5–8 days after ovulation in the mid-secretory phase of a normal human menstrual cycle.⁷ The process of embryo implantation consists of three stages, including apposition, adhesion, and invasion.^{8,9}

Adhesion molecules have been proven to be involved in the attachment of blastocyst to uterine epithelium. Previous studies have identified a group of integrins that play important roles on embryo implantation, including α v β 3, α 9 β 1, α v β 1, α 1 β 1, α 3 β 1, α 6 β 1, α v β 5, and α v β 6.^{10,11} Among these integrins, the integrin β 3 subunit

(β 3-integrin) has been proposed to have the most important role in both humans and mice. In the human endometrium, β 3-integrin is highly expressed in the luminal and glandular epithelium during the mid-secretory phase, while the aberrant expression of β 3-integrin is associated with infertility and recurrent pregnancy loss.^{12–14} The integrins have the ability to bind arginine-glycine-aspartic acid (RGD) sequences in extracellular ligands, while an intrauterine injection of RGD peptide or neutralizing antibody against β 3 reduces the number of implantation sites in mice.¹⁵

To date, only hysteroscopy to treat endometrial pathology and treatment of hydrosalpinges have been proven significantly beneficial for endometrial receptivity and incorporated in clinical standard care.¹⁶ Intrauterine administration of human chorionic gonadotropin, granulocyte colony stimulating factor or peripheral blood mononuclear cells have emerged as novel potential approaches to improve endometrial receptivity, while the treatment efficiency and underlying mechanism need to be demonstrated further.^{17–19} Over the last few decades, peptides have been recognized as a rapidly expanding therapeutic modality occupying the space between small molecules and antibodies.²⁰ Peptides are recognized for being highly selective and efficacious and, at the same time, relatively

safe and well tolerated. Preimplantation factor (PIF) is an embryo-specific peptide of 15 amino acids secreted by viable mammalian embryos, which establishes effective embryonic–maternal communication by regulating systemic and local immunity, leading to a pro-receptive environment prior to implantation.^{21–23} A Nur77-derived peptide has been shown to induce the apoptosis of cancer cells *in vitro* and in animals.^{24,25} We previously showed that Nur77 knockout mice were infertile due to impaired decidualization, but it not clear about the role of Nur77 on embryo-epithelium interaction.²⁶ Herein, we identified a Nur77 (also known as NR4A1 or TR3) derived peptide containing phosphorylated T366, a novel phosphorylation site mediated by mammalian sterile 20 (STE20)-like kinase 1 (Mst1, also known as KRS2 or STK4), promoted trophoblast–uterine epithelium adhesion *in vitro* and embryo implantation *in vivo* by regulating integrin expression. Both active Mst1 and phospho-Nur77 (T366) expression levels were increased in the mid-secretory endometrium than that in the proliferative endometrium, while decreased in the endometrium of women with RIF compared with the fertile controls, highlighting active Mst1 and phosphorylated Nur77 as promising biomarkers for endometrial receptivity.

Materials and methods

Patients and sample collection

Following the postovulatory rise in circulating progesterone levels, the endometrium becomes transiently receptive to embryo implantation.²⁷ Endometrial biopsy was performed through a mock cycle on the day that an embryo transfer would normally occur. Mid-secretory endometria timed on 6–8 days after exogenous progesterone treatment in the non-transfer cycle were obtained from 26 normal women and 26 women with RIF undergoing IVF-ET. Proliferative endometria were obtained from 12 normal women. The normal group was composed of women whose infertility was due to male factors and were confirmed to be fertile after their first IVF-ET treatment. RIF is defined as the absence of implantation after two consecutive cycles of IVF, intracytoplasmic sperm injection (ICSI) or frozen embryo

replacement cycles in which the cumulative number of transferred embryos is no less than four for cleavage-stage embryos and no less than two for blastocysts, with all embryos being of good quality as described previously.²⁸ All the patients were aged <35 years with regular ovulatory cycles of 28–32 days and normal BMI (<25 kg/m²) at time of biopsy, had normal endocrine profile including normal serum levels of FSH (<10 mIU/mL), LH (<10 mIU/mL) and estradiol (E2 < 50 pg/mL) on Day 3 of the menstrual cycle. Women with hydrosalpinx, endometriosis, or adenomyosis were excluded. The details of these patients are summarized in Table 1. The endometrial biopsies used for this study were obtained from women attending the Center for Reproductive Medicine of Nanjing Drum Tower Hospital (2013-408 081-01). All patients provided written informed consent.

Animals and treatments

A total of twenty adult female ICR (Institute of Cancer Research) mice were purchased from the Lab Animal Center of Yangzhou University (Yangzhou, China). To induce delayed implantation, mice were ovariectomized in the morning (08:00–09:00) on D4 of pregnancy and maintained with daily subcutaneous injections of progesterone (P4, 2 mg per mouse, MilliporeSigma) from D5 for three consecutive days (D5–D7); embryo implantation was triggered by the injection of oestradiol-17β (E2, MilliporeSigma) on D7 at 08:00.²⁹ Mice were randomly allocated to experimental groups in two-stages. Initially randomising an original allocation of sixteen mice, and then randomly allocating an additional four mice post-enlarging the sample size following a power analysis based on a priori assumptions. Saline or 20 μg peptide was injected into the uterus following the E2 trigger. E2 (7.5 ng) was injected into the sham group (n = 6 uteri), while E2 (3.75 ng) was injected into the intrauterine injection groups including saline group (n = 14 uteri), unphosphorylated peptide group (n = 7 uteri) and phosphorylated peptide group (n = 7 uteri). Implantation was checked via the blue dye method in mice 24 h after the E2 trigger, and the uterus was sampled for RNA-seq (n = 3 for saline treated uteri

Variables	For WB assay				For IHC assay			
	Normal proliferative (n = 6)	Normal mid-secretory (n = 14)	RIF mid-secretory (n = 14)	P value	Normal proliferative (n = 6)	Normal mid-secretory (n = 12)	RIF mid-secretory (n = 12)	P value
Age (y)	29.3 ± 2.3	30.1 ± 3.7	31.9 ± 2.1	0.15	29.3 ± 2.3	30.1 ± 3.7	31.9 ± 2.1	0.15
BMI (kg/m ²)	20.7 ± 2.2	21.2 ± 1.8	20.3 ± 2.3	0.65	20.7 ± 2.2	21.2 ± 1.8	20.3 ± 2.3	0.65
Basal FSH (IU/L)	7.8 ± 0.98	7.8 ± 0.96	7.2 ± 0.85	0.43	7.8 ± 0.98	7.8 ± 0.96	7.2 ± 0.85	0.43
Basal LH (IU/mL)	4.3 ± 1.3	4.1 ± 1.5	3.8 ± 1.3	0.73	4.3 ± 1.3	4.1 ± 1.5	3.8 ± 1.3	0.73
Basal E2 (pmol/mL)	35.7 ± 10.8	35.9 ± 16.0	38.9 ± 16.9	0.89	35.7 ± 10.8	35.9 ± 16.0	38.9 ± 16.9	0.89

Table 1: Clinical characteristics of women enrolled in the present study.

and $n = 3$ for phosphorylated peptide treated uteri) at 12 h after the E2 trigger. All steroid hormones (P4 and E2) were dissolved in sesame oil (MilliporeSigma) and injected subcutaneously. All animal experiments were approved by the Institutional Animal Care and Use Committee of Nanjing Drum Tower Hospital.

Cell culture and treatment

Ishikawa (RRID: CVCL_2529), HEK293T (RRID:CVCL_0063) and BeWo (RRID: CVCL_0044) cells were maintained as described previously.²⁶ The cell lines were verified by short tandem repeat analysis and routinely tested for mycoplasma contamination by PCR and confirmed negative in our lab as described previously.³⁰ For treatment with oestradiol and progesterone, cells were cultured in phenol red-free DMEM/F12 supplemented with 10% charcoal-stripped foetal bovine serum for 24 h before being treated with 10^{-8} M 17 β -oestradiol (#E2758, MilliporeSigma) and 10^{-6} M progesterone (#M1629, MilliporeSigma) for various durations. Cycloheximide (#508739, MilliporeSigma) was added for the indicated times at a final concentration of 50 μ g/mL for the protein degradation assay.

Peptides

The sequences of the examined peptides from Nur77 are as follows: unphosphorylated peptide, NH₂-GRKKR RQRRRPQANLLTSLVRA-COOH; phosphorylated peptide (pThr³⁶⁶), NH₂-GRKKRRQRRRPQANLL (pThr) SLVRA-COOH; mutant (Ala³⁶⁶), NH₂-GRKKRRQRR RPQANLLASLVRA-COOH. The β 3-integrin antagonist and the peptide control were cyclo (Arg-Gly-Asp-d-Phe-Lys) (cRGDFK) and cyclo (Arg-Gly-Glu-d-Phe-Lys) (cRGEfK), respectively. All peptides were synthesized (GenScript Biotech) at more than 98% purity, as verified by HPLC and mass spectrometry.

Construction of adenovirus

Adenoviruses harbouring Nur77 (Ad-Nur77), wild-type Mst1 (Ad-Mst1) and kinase activity-deficient Mst1 (Ad-Mst1-DN) were generated using AdMax (Microbix) as previously described.^{31,32} The siRNAs targeting Nur77 were purchased from Sangon Biotech and designed to target the following cDNA sequences: Nur77-1, CAGTCCAGCCATGCTCCTCT; Nur77-2, GGAAGATG CTGGGGATGTAT. The viruses were propagated in HEK293A cells and purified via CsCl₂ banding followed by dialysis against 20 mmol/L Tris-buffered saline with 10% glycerol.

Recombinant proteins purification

GST-Nur77-LBD and GST-Nur77-LBD^{T366A} fusion proteins were expressed in BL21 *Escherichia coli* using the pGEX4T-1 vector. For induction, 5 mL of Luria broth

medium (100 mg/mL ampicillin) was inoculated with a single colony. Three hundred microlitres of Pierce Glutathione Agarose (#16101, Thermo Scientific) (pre-treated with cold PBS) was added to the lysate supernatant and incubated with continuous mixing for 3 h at 4 °C, and the proteins were eluted with 300 μ l elution buffer (15 mM glutathione, 50 mM Tris-HCl, pH 8.0). After dialysis using Slide-A-Lyzer Dialysis Cassettes (#66380, Thermo Scientific) with 50 mM Tris-HCl (pH 7.5) +10% glycerol at 4 °C for 48 h, the proteins were divided into batches and stored at -80 °C.

Antibodies

Antibodies were purchased from the following companies: Mst1 (#3682; WB, 1:1000; IHC, 1:200), phospho-Mst1-Thr183 (#3681; WB, 1:1000; IHC, 1:200), phospho-Nur77-Ser351 (#5095; WB, 1:1000), Flag (#14793; WB, 1:1000), Myc (#2276; WB, 1:1000; IF, 1:100) (all from Cell Signalling Technology), phospho-threonine (#P6623; WB, 1:500), phosphoserine (#P5747; WB, 1:1000) (all from Millipore Sigma), Nur77 (#ab48789, Abcam; WB, 1:1000; IHC, 1:200), HOXA10 (#sc-17158; WB, 1:1000), and phospho-Nur77-Ser341 (#sc-16991; WB, 1:1000) (all from Santa Cruz Biotechnology, Inc.), β 3-integrin (#BS3660; WB, 1:1000), GAPDH (#AP0063; WB, 1:2000) (all from Bioworld Technology, Inc.), FAK (#CY5464; WB, 1:1000), phospho-FKA-Y397 (#CY5464; WB, 1:1000) (all from Abways Technology, Inc.). The phosphorylation state-specific antibody against phospho-Nur77-Thr366 was provided by Nanjing Peptide Biotech (WB, 1:400). As brief, the synthetic phosphorylated peptide ANLLT^PSLVRA was subjected to immunization of rabbits, following with a two-step affinity purification with a non-phosphorylated peptide column and a phosphorylated peptide column to get the polyclonal antibody against phospho-Nur77-Thr366.

Western blot analysis

Tissues and cells were homogenized in whole-cell lysis buffer (50 mM Tris-HCl [pH 7.6], 150 mM NaCl and 1.0% NP-40) containing a protease inhibitor cocktail (#11697498001, Roche Life Science) and a phosphatase inhibitor cocktail (#P5726, MilliporeSigma). Proteins were resolved by 10% SDS-PAGE gel and transferred onto PVDF (polyvinylidene difluoride) membranes (#03010040001, Millipore), then incubated with primary antibodies followed by a goat anti-rabbit (#BS13278; 1:10000) or anti-mouse (#BS12478; 1:10000) secondary antibody (Bioworld Technology, Inc.) conjugated with HRP. Detection was performed using an enhanced chemiluminescence kit (#32106, MilliporeSigma). Semiquantitative analysis was performed by densitometry, calculating the ratio of target protein(s) to GAPDH (ImageJ version 1.52, NIH software). Protein levels were equilibrated with Protein Assay Reagent (Bio-Rad Laboratories).

Co-immunoprecipitation

HEK293 cells were transiently transfected with the indicated plasmids. Both HEK293 cells and Ishikawa cells were lysed in buffer containing 1% NP-40, 150 mmol/L NaCl, 50 mmol/L Tris (pH 8), 100 μ mol/L EDTA and protease inhibitors. The coimmunoprecipitation of Mst1 and Nur77 was performed essentially as we described previously.¹⁴ The following antibodies were used for immunoprecipitation: anti-Myc agarose beads (#20168, Invitrogen), anti-Flag M2 agarose beads (#A2220, MilliporeSigma) or anti-Mst1 (#3682, Cell Signalling Technology) followed by Protein G agarose beads (Roche Life Science).

Immunohistochemistry

Endometrial tissues were fixed in 10% neutral-buffered formalin for 24 h and then routinely processed and embedded in paraffin. Tissue sections were deparaffinized, rehydrated, then subjected to antigen retrieval by boiling in 10 mM citrate buffer (pH 6.0) for 10 min. The sections were incubated overnight in primary antibody at 4 °C, followed with immunohistochemical staining kits (Zhongshan Golden Bridge). Control sections were run concurrently with the experimental sections using nonspecific rabbit IgG (#sc2027, Santa Cruz Biotechnology, Inc.). Digital images were captured using a Leica DM 2000 microscope and LAS Core software (Leica Microsystems Limited, Wetzlar, Germany). Quantitative analysis of the relative protein expression levels in the epithelial cells and stromal cells of endometrium samples were determined according to the integrated optical density (IOD) of the digital images ($\times 400$) using Image-Pro Plus System 6.0 (Media Cybernetics, Inc., Silver Spring, MD, USA) in a blinded fashion as described previously.³³ Signal density data for the tissue areas were obtained from three randomly selected fields of view and subjected to statistical analysis.

Immunofluorescent staining

Ishikawa cells grown on 8-well microscope slides (Millipore) were transfected with Flag-Nur77^{K164R} together with the Myc-Mst1 expression plasmid. After 48 h, cells were fixed with 4% paraformaldehyde in PBS for 20 min, washed in PBS and treated with 0.5% Triton X-100 in PBS for 10 min. Protein blocking with 3% BSA in PBS was performed for 30 min at room temperature. The cells were subsequently incubated with anti-Flag or anti-Myc antibodies overnight at 4 °C, followed by incubation with secondary anti-rabbit Cy3 (#111165, Jackson ImmunoResearch) and anti-mouse Cy2 (#115225, Jackson ImmunoResearch) antibodies. The slides were counterstained with DAPI and imaged on an Olympus FV1000 confocal microscope (Olympus Corporation, Shinjuku).

In vitro kinase assay

HEK293 cells transfected with Flag-Nur77 were serum starved for 6 h before harvest, and then Flag-Nur77 was immunoprecipitated with an anti-Flag antibody. Kinase assays were carried out as described with some modifications.^{34,35} The immunoprecipitated complexes were washed 2 \times with lysis buffer and once with wash buffer (40 mM HEPES pH 7.6, 10 mM MgCl₂, 1 mM EGTA, 1 mM DTT) and then incubated with active Mst1 (Millipore) in kinase buffer (40 mM HEPES pH 7.6, 10 mM MgCl₂, 1 mM EGTA, 1 mM DTT, 2.5 mM β -glycerophosphate, 200 μ M ATP) for 30 min at 30 °C. The reactions were stopped by the addition of 5 \times Laemmli sample buffer, heating at 95 °C for 5 min, subjected to SDS-PAGE and blotted with the indicated antibodies. For phosphorylation of GST-Nur77-LBD and GST-Nur77-LBD^{T366A}, the reactions were subjected to autoradiography.

Phos-tag SDS-PAGE

For analysis of Nur77 phosphorylation, samples of tissue extracts in SDS-gel sample buffer were subjected to phosphate affinity SDS-PAGE using an acrylamide-pendant phosphate-binding tag (Phos-tagTM) with Mn²⁺ as previously described.^{36,37} Standard Tris-Cl buffered stacking (4.5% w/v acrylamide) and separating (6% w/v acrylamide, 50 μ M Phos-tagged acrylamide, 100 μ M MnCl₂) gel recipes were applied. Electrophoresis was performed under constant current conditions (30 mA/gel) until the BPB reached the bottom of the resolving gel. For transfer of gel-separated proteins to PVDF membranes, gels were pretreated with washing in methanol-free transfer buffer with 5 mM EDTA for 10 min twice to remove bivalent cations. Immunoblotting was performed with primary antibodies against Nur77 (#3960, Cell Signaling Technology). Western blots of Phos-TagTM gels cannot be used to make MW assignments.

LC-MS/MS analysis

Protein bands were excised from Coomassie-stained gels. Proteins were isolated, digested, and labelled with iTRAQ reagents. LC-MS/MS was performed with a Triple TOF 5600 System (AB SCIEX) in the Translational Medicine Core Facilities, Medical School of Nanjing University as described.³⁸ The raw data used for proteomic profiling are provided in [Supplementary Datasheet 1 and 2](#).

Luciferase reporter assay

The synthetic triple sequence repeats of NBRE were cloned into the pGL3-basic luciferase reporter plasmid (#E1751, Promega) and sequenced to confirm the resulting plasmid. Preconfluent (60%) Ishikawa cells in 12-well plates were transfected with the indicated

plasmids. Cells were harvested, and the luciferase activities were analysed after 48 h using a Dual-Luciferase Assay System (#E2940, Promega). Luciferase activity was measured using a luminescence counter (Berthold Technologies) according to the manufacturer's instructions. For normalization according to the transfection efficiency, firefly luciferase activity was normalized to the corresponding *Renilla* luciferase activity.

Avidin-biotin conjugate DNA precipitation assay

The biotin-labelled DNA probes were synthesized by Sangon Biotech. The primers contained triple repeats of NBRE and were biotinylated at the 5'-end. The primer sequences were as follows: forward: biotin-5'-GGGAAAGGTCAAAGGTCAAAGGTCAAAGTCCCG-3'; reverse: 5'-CGGGACTTTGACCTTTTACCTTTTACCTTTTCC-3'. Double-stranded oligonucleotides were designed based on the β 3-integrin promoter sequence (-6981 to -6952 bp): β 3-integrin wild-type forward: 5'-biotin-GGAGACAGTAGAAAGGTCAAGTCGTTTCCAG-3', and reverse: 5'-CTGAAACGACTGACCTTCTACTGTCTCC-3'; and β 3-integrin mutant forward: 5'-biotin-GGAGACAGTAGACATTTTCAAGTCGTTTCCAG-3', and reverse: 5'-CTGAAACGACTGAAATGTCTACTGTCTCC-3'. ssDNA was thermally annealed to form dsDNA prior to pull-down experiments. Cell lysates derived from Ishikawa cells transfected with the indicated plasmids or adenovirus were incubated with 500 pmol of double-stranded DNA and then subjected to pull-down using streptavidin agarose beads (MilliporeSigma). Proteins were resolved via SDS-PAGE and probed with an anti-Flag antibody.

Adhesion assay for BeWo spheroid and mouse embryo adhesion to Ishikawa cells

Multicellular spheroids of human choriocarcinoma BeWo cells and mouse blastocysts with endometrial Ishikawa cells were used as *in vitro* models of adhesion as described previously.^{39,40} Briefly, a single-cell suspension of BeWo cells was transferred to a Petri dish coated with the antiadhesive polymer poly-2-hydroxyethyl methacrylate (#P3932, MilliporeSigma) to induce the formation of BeWo spheroids that were 150–200 μ m in diameter. Simultaneously, a confluent monolayer of Ishikawa cells was infected with the indicated adenovirus vectors for 48 h or treated with the indicated peptides (cRGDfK and cRGEfK: 2 μ g/mL; Nur77-derived peptides: 4 μ g/mL) for 24 h. Fifty spheroids per chamber were transferred onto the confluent monolayer of Ishikawa cells. After the spheroids were incubated for 1.5 h, the attached spheroids were counted, and the adhesion rate was expressed as a percentage of the total number of spheroids (% adhesion). Similarly, collected mouse blastocysts were

transferred to Ishikawa cells treated with the phosphorylated peptide (pThr³⁶⁶) in a 24-well culture plate, with 5 blastocysts per well. After 24 h, a standardized plate movement protocol was implemented to measure embryo attachment stability.

RNA-seq and data analysis

Total RNA was isolated from the mouse uterus following the standard TRIzol extraction protocol. cDNA library generation, Illumina sequencing, alignment of high-quality reads to the mouse genome (mm10) (GRCh38) using HISAT2, and transcriptome assembly using StringTie were performed by Gene Denovo Biotechnology. The DESeq2 (v1.29.12) package was used to normalize count data and for differential gene expression ($\log_2FC > 1$, P value < 0.05) analysis in the R program (R version 4.0.2). Gene set enrichment analysis (GSEA) was performed using GSEA software v4.1.0. The significantly ($P < 0.05$) regulated genes were extracted for downstream pathway analyses using Metascape.⁴¹ The graphics were drawn using the ggplot2 package in R software.

Statistical analysis

Each experiment was repeated at least 3 times. All values are expressed as the mean \pm SD. Two-tailed unpaired Student's *t* tests were used for comparisons of two groups. No blinding method was used for animal studies. A priori power analysis for sample size calculations was made with "resource equation" based on law of diminishing return. Following the formula: $E = \text{total number of samples} - \text{total number of groups}$, the value of E was set as more than 20.⁴² ANOVA with Tukey's multiple comparisons test was applied for experiments involving more than two groups. The Mann-Whitney test was used to test the stability of embryo attachment to Ishikawa cells between the two groups. Pearson correlation analysis was used to assess the relationship between the protein levels of pNur77 (T366) and β 3-integrin. A P value < 0.05 was considered statistically significant.

Results

Mst1 is involved in establishing endometrial receptivity dependent on the kinase activity

Treatment with oestradiol (E_2) and progesterone (P_4) induced Ishikawa cells, a well-differentiated endometrial adenocarcinoma cell line, to enter the receptive stage, as characterized by increased levels of HOXA10 and β 3-integrin.⁴³ The protein levels of Mst1 and catalytically active Mst1 (phos-T183-Mst1, pMst1) were markedly increased at the 12 h time point, while the levels of active Mst1 and β 3-integrin were decreased after 72 h of treatment (Fig. 1A). Further, we found

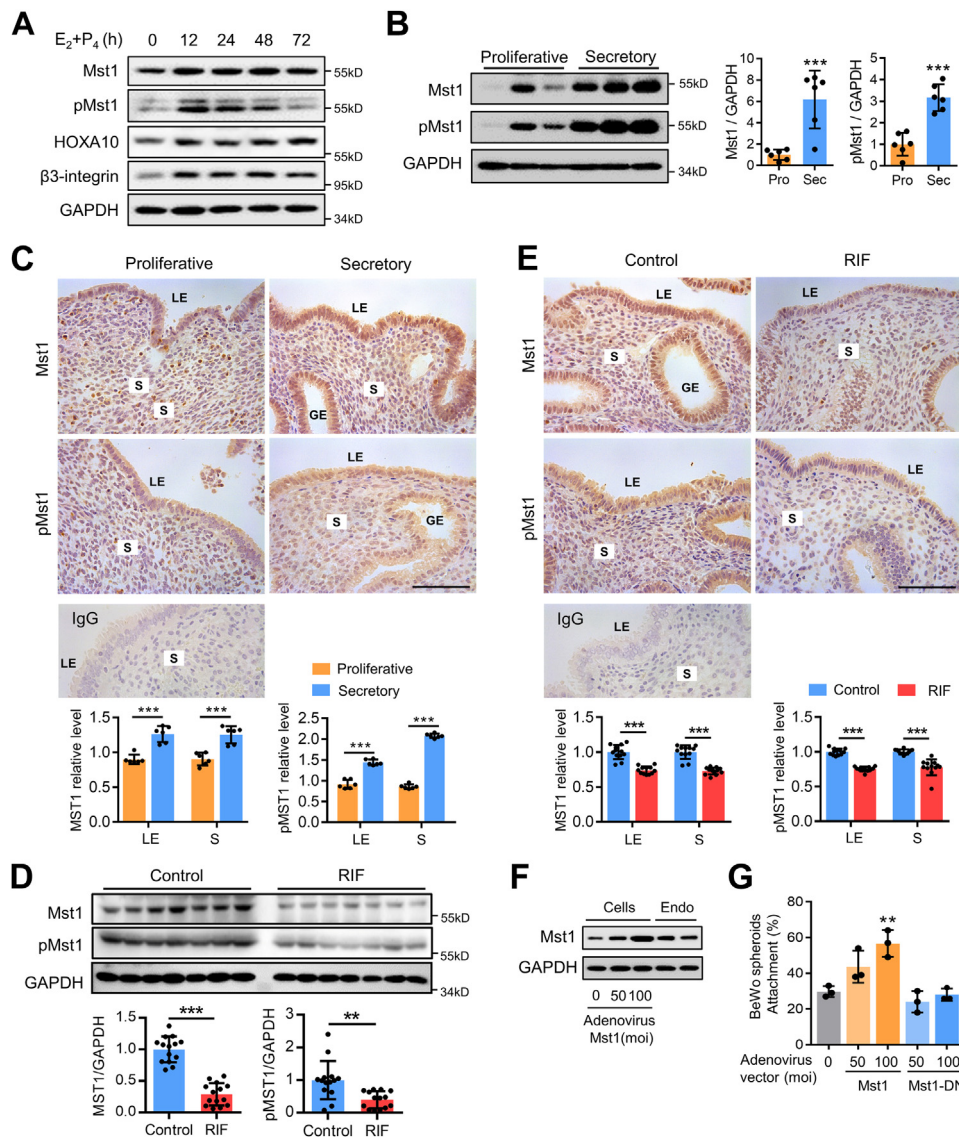


Fig. 1: Mst1 is involved in establishing endometrial receptivity dependent on the kinase activity. (A) Western blot analysis of Mst1, pT183-Mst1, Nur77 and β 3-integrin protein levels in Ishikawa cells treated with oestradiol (E₂; 10⁻⁸ M) and progesterone (P₄; 10⁻⁶ M) for 0, 12, 24, 48 and 72 h. (B) Western blot analysis of Mst1 and pT183-Mst1 protein levels in mid-secretory endometrium (n = 6) and proliferative endometrium (n = 6) from normal fertile women. Data are presented as the ratio of the target protein level to the level of GAPDH. (C) Immunostaining analysis of Mst1 and pT183-Mst1 protein expression in proliferative endometrium (n = 12) versus mid-secretory endometrium (n = 12) from normal fertile women. (D) Western blot analysis of Mst1 and pT183-Mst1 protein levels in mid-secretory endometrium from infertile women with RIF (n = 14) and normal controls (n = 14). Data are presented as the ratio of the target protein level to the level of GAPDH. (E) Immunostaining analysis of mid-secretory endometrial Mst1 and pT183-Mst1 and Nur77 protein expression in women with RIF (n = 12) versus normal controls (n = 12). (F) Western blot assay of Ishikawa cells transfected with adenovirus harbouring Mst1 and mid-secretory human endometrium from normal controls. (G) Adhesion experiments with BeWo spheroids attached to the Ishikawa cell monolayer transfected with the indicated adenovirus harbouring Mst1 or domain-negative Mst1 (Mst1-DN). LE, luminal epithelium; GE, glandular epithelium; S, stroma. Scale bars, 100 μ m. Mean \pm SD. **P < 0.01, ***P < 0.001, Student's t test in B, E and F, ANOVA with Tukey's multiple comparisons test in D.

that the expression of Mst1 and pMst1 were greater in the mid-secretory endometrium than in the proliferative endometrium, especially in the endometrial luminal epithelial cells, while reduced in the luminal

epithelial cells of mid-secretory endometrium from women with RIF than that in the normal controls (Fig. 1B–E). To determine the role of Mst1 in embryo-epithelium interaction, we cocultured confluent

Ishikawa cells with BeWo spheroids⁴⁰ and found that Mst1 overexpression dose-dependently promoted BeWo spheroids adhesion, but the kinase domain negative Mst1 (Mst1-DN) did not (Fig. 1F and G). The above results indicated that Mst1 activation in the luminal epithelial cells of receptive endometrium promoted trophoblast–uterine epithelium adhesion *in vitro*, which was impaired in the endometrium of women with RIF.

Mst1 promotes the transcriptional activity of Nur77 by interacting with Nur77

Our previous yeast two hybrid assay using Nur77 as bait identified Mst1 as a Nur77 interacting protein (data not shown). Co-immunoprecipitation assay with the Nur77 antibody confirmed the interaction between the endogenous Nur77 and Mst1 protein in the human endometrium (Fig. 2A). Both Mst1 and kinase domain negative Mst1 (Mst1-DN) interacted with Nur77 in the Ishikawa cells (Fig. 2B and C). Further, we found that Nur77 interacted with both full-length Mst1 (Mst1-FL) and N-terminal Mst1 with kinase domain (Mst1-NT), but not the C-terminal Mst1 with regulatory domain (Mst1-CT) (Fig. 2D). Interestingly, Mst1 associated with all the N-terminal Nur77 with transactivation domain (Nur77-TAD), Nur77 with DNA-binding domain (Nur77-DBD) and Nur77 with ligand-binding domain (Nur77-LBD) (Fig. 2E). However, we did not find any interaction of Mst1 with the Nur77 paralogous proteins NR4A2 and NR4A3 (Fig. S1).

We next investigate the role of Mst1 on Nur77. Over-expression of Nur77 promoted BeWo spheroids attachment, which was enhanced by wild type Mst1 (Fig. 2F and G). We found that Mst1 did not increase the mRNA level of *Nr4a1* (gene name for Nur77), instead increased the protein level of Nur77 by approximately 75% at 8 h after CHX treatment (Nur77 vs Nur77 + Mst1 = 45% vs 75%, $P < 0.01$) (Fig. 2H and I). Mst1 increased the transcriptional activity of Nur77 by approximately 25% ($P < 0.01$), indicated by increased luciferase activity driven by nerve growth factor-induced B factor response element (NBRE) (Fig. 2J). Furthermore, an avidin-biotin conjugate DNA precipitation assay showed that Mst1 promoted the DNA binding of Nur77 to NBRE (Fig. 2K). Treatment with E_2 and P_4 induced the transcriptional activity of Nur77 in Ishikawa cells, which was blocked by knockdown of Mst1 (Fig. 2L), indicating the Mst1 mediated the regulatory effect of estrogen and progesterone on Nur77 molecular function. However, Mst1-DN had no these promoting effect on Nur77. Together, these data indicated that Mst1 interacted with Nur77, and regulate the transcriptional activity of Nur77 dependent on its kinase activity, prompting us to examine whether Mst1 directly phosphorylates Nur77.

Mst1 phosphorylates Nur77 at threonine 366

The expression of Nur77 and total phosphorylation level of Nur77 was higher in the mid-secretory endometrium than that in the proliferative endometrium (Fig. 3A and B). *In vitro* kinase assay was conducted with the immunoprecipitated Nur77 protein and the recombinant active Mst1 protein, leading to the auto-phosphorylation of Mst1 and a marked phosphorylation of Nur77 detected by anti-phosphothreonine IgG (Fig. 3C). The chromatography-tandem mass spectrometry (LC/MS/MS) were further used to identify potential phosphorylation sites in Nur77, and the sequence coverage of Nur77 in the LC-MS/MS assay was 76.6% (Fig. 3F and G). The phosphorylation modifications of threonine were found only at Thr-27 and Thr-366, in which only phosphorylation of Thr-366 was induced by active Mst1 specifically (Fig. 3H and Fig. S2A). As Thr-366 was included in the LBD domain of Nur77, we purified the Nur77-LBD and phospho-dead mutant Nur77-LBD^{T366A} recombinant proteins and found that active Mst1 phosphorylated Nur77-LBD but not Nur77-LBD^{T366A} (Fig. 3G and Fig. S2B). Although Nur77^{T366A} colocalizes with Mst1 in the nucleus of Ishikawa (Fig. S2C), Nur77^{T366A} showed decreased NBRE-luciferase reporter activity (Nur77^{WT} vs Nur77^{T366A} = 9.9-fold vs 7.1-fold, $P < 0.01$) and protein stability compared with Nur77 (Fig. 3H and Fig. S2D). It was further confirmed that Mst1 promoted the transcriptional activity of Nur77 but not Nur77-LBD^{T366A} (Fig. 3I). All the above data showed that Mst1, as a novel kinase that phosphorylates Nur77 at Thr-366, played an important role in regulating the transcriptional activity of Nur77 at the post-translational level.

A phosphorylated peptide derived from Nur77 promotes endometrial receptivity

We speculated that a phosphorylated peptide containing threonine 366 of Nur77 may play a key role on the embryo-epithelium interaction. A transactivator of transcription (TAT) peptide was fused with the peptide corresponding to residues 362–371 of Nur77 (Fig. 4A). We found that the Nur77-derived peptide containing phosphorylated threonine 366 (Peptide-pThr³⁶⁶) promoted the transcriptional activity of Nur77 in Ishikawa cells, but Peptide-Wt had no such promoting effect (Fig. 4B). We further found that peptide-pThr³⁶⁶ was the only peptide that promoted BeWo spheroid adhesion by approximately 10% compared with peptide-WT and a phosphorylation-defective mutant peptide (Peptide-Ala366) (Fig. 4C). By using an *in vitro* model of mouse embryo adhesion, we further showed that embryos incubated with peptide-pThr³⁶⁶-treated Ishikawa cells exhibited a higher attachment score [4 (2–4); median (interquartile range), $n = 34$] than the control group [3 (2–4), $n = 34$] ($P < 0.01$) (Fig. 4D). We next determined

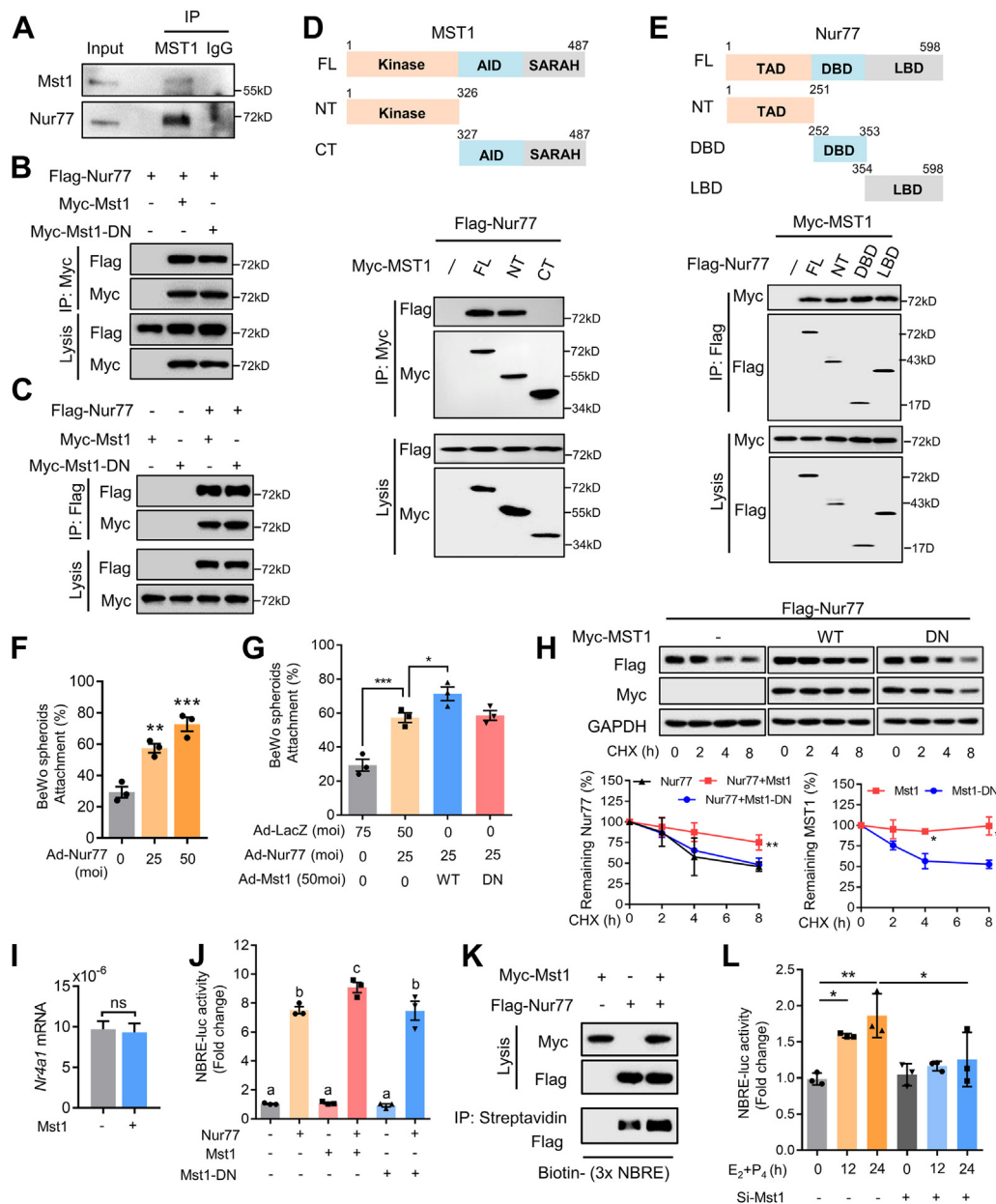


Fig. 2: Mst1 promotes the transcriptional activity of Nur77 by interacting with Nur77. (A) Extracts from normal mid-secretory endometrium were subjected to coimmunoprecipitation with an Mst1 antibody or Rabbit IgG control, and Western blot analysis of the precipitate was performed for the Nur77 protein. (B, C) Extracts from HEK293T cells transfected with the indicated plasmids were subjected to immunoprecipitation with a Myc (B) or Flag (C) antibody, then for Western blot analysis. (D) Diagram of different truncated protein of Mst1 and Nur77. (E, F) Extracts from HEK293T cells transfected with the indicated plasmids loading truncated Mst1 or Nur77 were used for IP following with Western blot analysis. (F, G) Adhesion experiments with BeWo spheroids attached to the Ishikawa cell monolayer transfected with the adenovirus harbouring Nur77 at different concentrations (F), and Mst1 or Mst1-DN (G). (H) Ishikawa cells transfected with Flag-Nur77 and Myc-Mst1 or Mst1-DN were treated with CHX and then subjected to Western blot assays. The level of the remaining Nur77 was normalized to that of GAPDH and plotted relative to the level at the 0-h time point. (I) The expression of Nr4a1 mRNA was detected in Ishikawa cells transfected with Mst1 or not. (J) Ishikawa cells transfected with Flag-Nur77 and Myc-Mst1 or kinase activity-deficient Mst1 (Mst1-DN), as indicated, were subjected to the detection of NBRE-luciferase activity. (K) Ishikawa cell extracts were incubated with a biotinylated DNA probe containing three NBRE repeats, enriched by streptavidin Sepharose beads, then subjected to Western blot analysis using a Flag antibody. (L) Ishikawa cells were treated with E₂ and P₄ after the knockdown of Mst1, and NBRE-luciferase activity was detected. Mean \pm SD. * $P < 0.05$, ** $P < 0.01$, *** $P < 0.001$, columns labelled with different letters show differences at the $P < 0.05$ level. Student's *t* test in H and I, ANOVA with Tukey's multiple comparisons test in F, G, J and L.

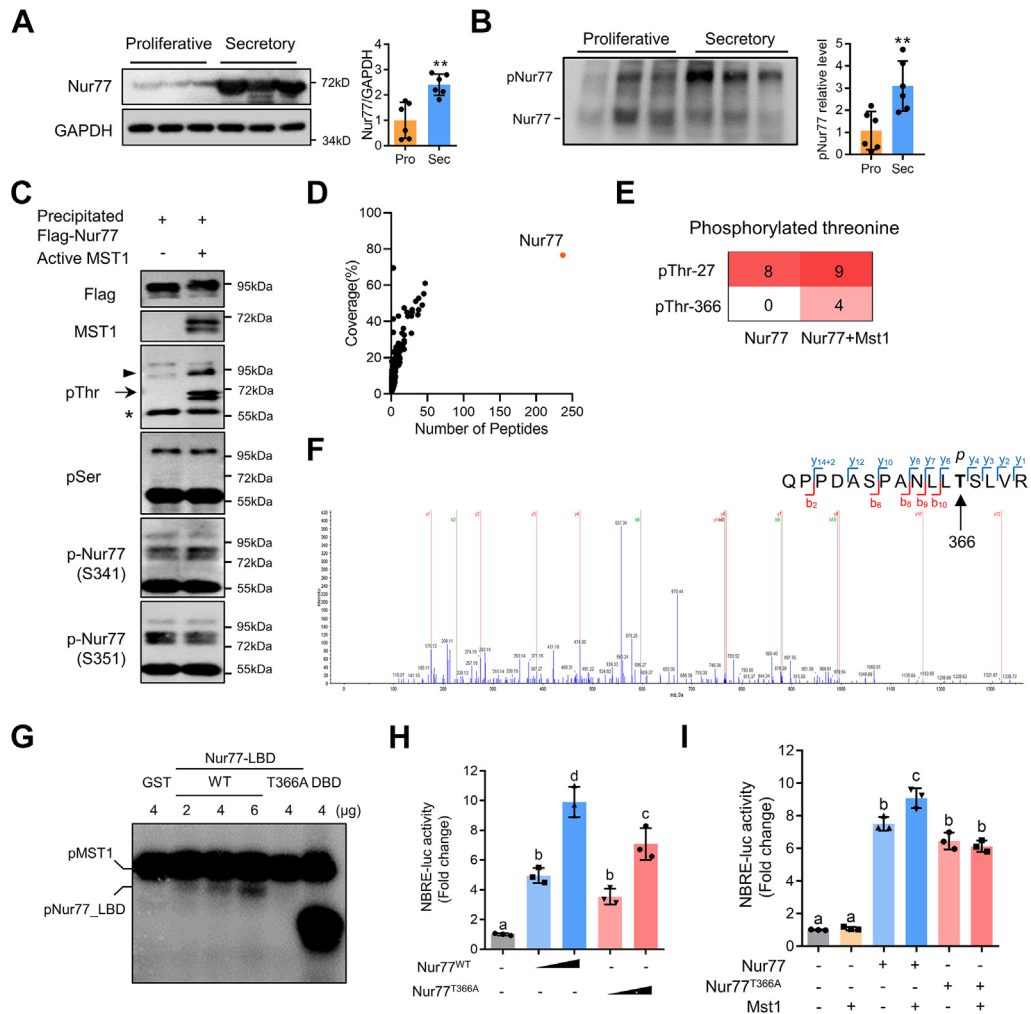


Fig. 3: Mst1 promotes Nur77 transcriptional activity by phosphorylating directly Nur77 at threonine 366. (A) Western blot analysis of Mst1 and pT183-Mst1 protein levels in mid-secretory endometrium (n = 6) and proliferative endometrium (n = 6) from normal fertile women. (B) Phospho-tag SDS-PAGE analysis of Nur77 and phosphorylated Nur77 protein in mid-secretory endometrium (n = 6) and proliferative endometrium (n = 6) from normal fertile women. (C) An *in vitro* phosphorylation assay was conducted by incubating precipitated Flag-Nur77 with recombinant active Mst1 for 30 min at 30 °C. Western blot analysis shows a phospho-Nur77 band identified by a phospho-threonine (pThr) antibody. (D) Identified peptide top hits from LC-MS/MS analysis. (E) The number of peptides containing phosphorylated threonine in the Nur77 plus active Mst1 group. (F) Mass spectrum graph showing the phosphorylation of Nur77 at Thr366. (G) An *in vitro* phosphorylation assay was conducted by incubating recombinant GST-Nur77-LBD or GST-Nur77-LBDT366A with recombinant active Mst1. (H) Ishikawa cells transfected with Nur77WT or Nur77TT366A were subjected to the detection of NBRE-luciferase activity. (I) Ishikawa cells transfected with Flag-Nur77 or Nur77TT366A and Myc-Mst1 were subjected to the detection of NBRE-luciferase activity. Mean ± SD. *P < 0.05, **P < 0.01, columns labelled with different letters show differences at the P < 0.05 level. Student's t test in A, ANOVA with Tukey's multiple comparisons test in H and I.

the effect of peptide-pThr³⁶⁶ on embryo implantation in a delayed implantation mouse model²⁹ (Fig. 4E). The sham group triggered with 7.5 ng E2 showed the highest implantation rate, while the saline group triggered with 3.75 ng E2 showed a poor implantation rate. Peptide-Wt injection slightly, but not significantly, increased the implantation rate, whereas Peptide-pThr³⁶⁶ injection significantly increased the implantation rate (4 vs 1.4, P < 0.01) compared with the saline group (Fig. 4F and G). Together, these results demonstrated that

peptide-pThr³⁶⁶ promotes trophoblast–uterine epithelium adhesion *in vitro* and embryo implantation *in vivo*, indicating the improvement of Peptide-pThr³⁶⁶ on endometrial receptivity.

Peptide-pThr366 from Nur77 promotes integrin expression in the endometrial epithelium

To elucidate the potential molecular mechanism underlying the peptide-pThr³⁶⁶-mediated promotion of

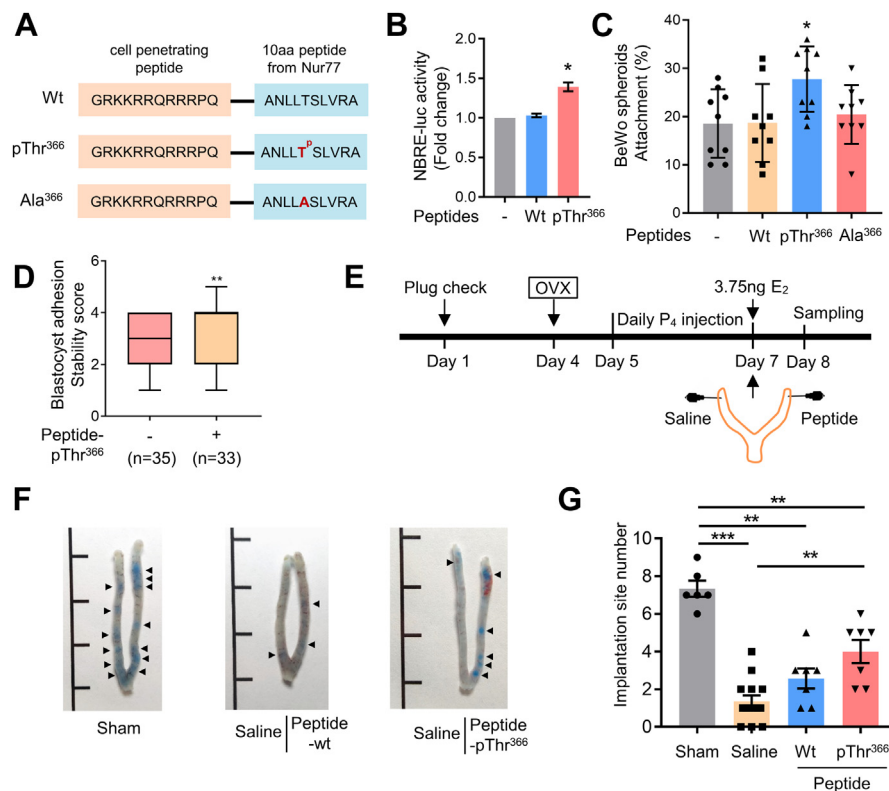


Fig. 4: A phosphorylated peptide derived from Nur77 promotes endometrial receptivity. (A) Schematic representation of Nur77-derived peptides: unphosphorylated peptide (Wt), phosphorylated peptide (pThr366) and mutant peptide (Ala366). (B) Ishikawa cells incubated with wt or pThr366 were subjected to the detection of NBRE-luciferase activity. (C) Adhesion experiments with BeWo spheroids attached to the Ishikawa cell monolayer treated with the indicated peptide at 4 $\mu\text{g}/\text{mL}$. (D) Adhesion experiments with mouse embryos attached to the Ishikawa cell monolayer treated with 4 $\mu\text{g}/\text{mL}$ Peptide-pThr366. Data are the median with the interquartile range of three independent experiments; boxes indicate quartiles, and whiskers indicate the range. (E–G) Delayed implantation in mice was triggered by E2 injection, followed by the intrauterine injection of saline ($n = 14$ uteri), Peptide-Wt ($n = 7$ uteri) or Peptide-pThr366 ($n = 7$ uteri), nothing was injected in the sham group ($n = 6$ uteri). After 24 h, mice were sacrificed by cervical dislocation to check implantation via the blue dye method. * $P < 0.05$, ** $P < 0.01$, *** $P < 0.001$. ANOVA with Tukey's multiple comparisons test in B, C and G, and the Mann-Whitney test was used in D.

endometrial receptivity, we collected uterine samples for RNA sequencing at 12 h after peptide injection (20:00, several hours before blastocyst implantation) when the mice uterus enter receptive phase⁴⁴ (Fig. 5A). The peptide group included a total of 1082 differentially expressed genes, among which 724 were upregulated and 358 were downregulated (Fig. 5B). GO pathway analysis showed that the upregulated genes of the peptide group were enriched in multiple pathways, including the “Regulation of cell adhesion” and “Integrin-mediated signalling pathway”, which are associated with the process of trophoblast–uterine epithelium adhesion (Fig. 5C). However, the analysis of downregulated genes focused on the pathways related to DNA replication and cell proliferation, indicating the decreased proliferation of endometrial epithelial cells, which is necessary for the maturation of endometrial epithelial cells and initiation of epithelium-embryo adhesion⁴⁵ (Fig. 5D). Gene set enrichment analysis

(GSEA) showed that the “Integrin-mediated signalling” gene set was significantly enriched in the Peptide-pThr³⁶⁶ group (FDR = 1.43E-4) (Fig. 5E). The expression of *Itgb1*, *Itgb3*, *Itga1* and *Itga5* was upregulated in the peptide-pThr³⁶⁶ group compared with the saline group, and the protein expression of $\beta 3$ -integrin was significantly increased in the epithelial cells of the uterus treated with peptide-pThr³⁶⁶ (Fig. 5F–H, Fig. S3). Interestingly, *Lif*, which is a crucial secretory factor from the glandular epithelium that induces the uterus to become receptive to implantation,⁴⁶ was markedly increased in the Peptide-pThr³⁶⁶ group (Fig. 5I). In addition, the mRNA expression of *Nr4a1* was increased in the peptide-pThr³⁶⁶ group, indicating that peptide-pThr³⁶⁶ promoted embryo implantation partly by inducing Nur77 expression (Fig. 5J). The above results suggest that Peptide-pThr366 derived from Nur77 promotes endometrial receptivity by regulating the integrin expression in the endometrial epithelial cells.

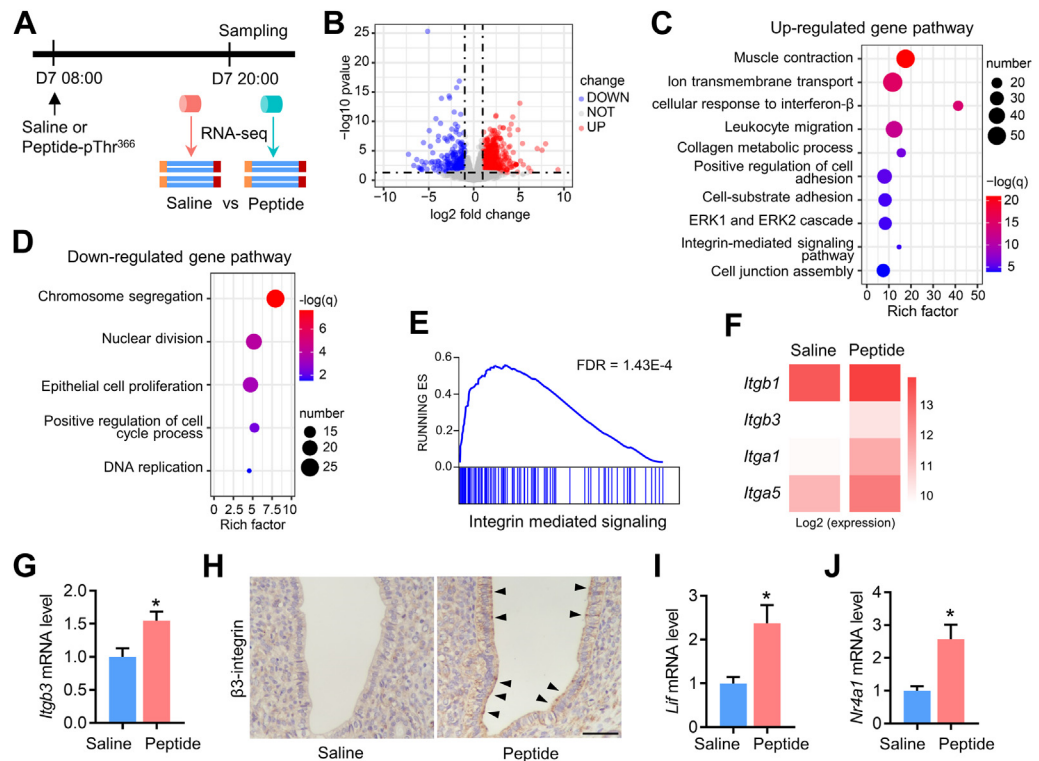


Fig. 5: Peptide-pThr366 from Nur77 promotes integrin expression in the endometrial epithelium. (A) Delayed implantation in mice was triggered by E2 injection, followed by the intrauterine injection of saline (n = 3 uteri) or peptide-pThr366 (n = 3 uteri). After 12 h, uteri were sampled for RNA-seq analysis. (B) Volcano plot of differentially expressed genes showing $P < 0.05$ and a log fold change >0.45 are highlighted in light blue and light red, respectively. (C, D) Metascape pathway analysis of upregulated genes (C) and downregulated genes (D). (E) The “Integrin-mediated signalling” gene set was enriched in the peptide group according to GSEA. (F) The expression of *Itgb1*, *Itgb3*, *Itga1* and *Itga5* was increased in the peptide group. Data are shown as log₂-normalized read counts. (G, H) qRT-PCR data of *Itgb3* mRNA levels and IHC assay of β 3-integrin protein levels between the control and peptide group. (I, J) qRT-PCR data of the expression of *Lif* and *Nr4a1* between the control and peptide group. Mean \pm SD. * $P < 0.05$ by Student’s t test.

Mst1 mediated phosphorylation of Nur77 regulates epithelium-embryo adhesion via β 3 integrin/FAK

Nur77 regulates gene expression by directly binding to NBRE, which was found in the promoter region of β 3-integrin (–6981 to –6952). Our results showed that Flag-tagged Nur77 strongly bound to the β 3-integrin promoter containing the AAAGGTCA sequence but not to its respective mutant containing the TGAAATGT sequence (Fig. 6A). Treatment with E2 and P4 increased the expression of β 3-integrin and induced FAK activation, which was inhibited by the knockdown of Nur77 (Ad-siNur77) using RNA interference (Fig. 6B and C). In addition, Mst1 increased the protein levels of β 3-integrin and phosphorylated FAK, which was blocked by knockdown of Nur77 (Fig. 6D and E). The RGD motif has been proven to bind to β 3-integrin, and the treatment of an Ishikawa cell monolayer with the RGD peptide inhibited BeWo-Ishikawa adhesion (Fig. S4). Furthermore, we found that the facilitation of BeWo-Ishikawa adhesion by Nur77 was blocked by the RGD peptide (by 27%, $P < 0.001$) but not by the mutant RGE

peptide (Fig. 6F). All these data showed that the phosphorylation of Nur77 mediated by Mst1 promoted epithelium-embryo adhesion by activating β 3 integrin/FAK signalling pathway.

Impaired phosphorylation of Nur77 in the endometrium of women with unexplained RIF

Based on the above results, we further determined the phosphorylation level of Nur77 in the endometrium of women with RIF. We found that the protein expression level of Nur77 was reduced in both of the luminal epithelial cells and stromal cells of mid-secretory endometrium from women with RIF (n = 12) than that in the normal controls (n = 12) (Fig. 7A). The Western blot assay further confirmed that the protein level of Nur77 were decreased by 59% ($P < 0.001$) in the mid-secretory endometrium from women with RIF (n = 14) than that in the normal controls (n = 14) (Fig. 7B). The Mn²⁺-Phos-tag SDS-PAGE assay confirmed that the total phosphorylation level of Nur77 was disrupted in the

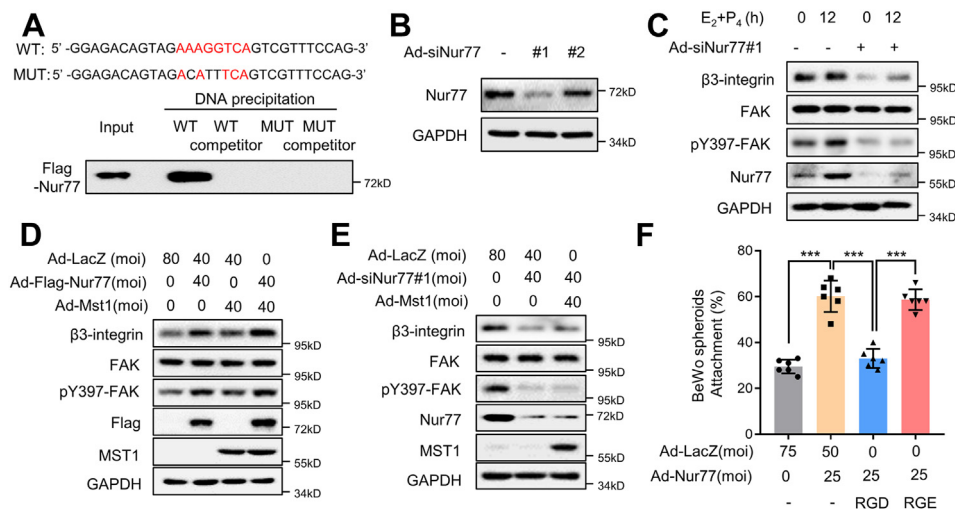


Fig. 6: Mst1 mediated phosphorylation of Nur77 regulates epithelium-embryo adhesion via $\beta 3$ integrin/FAK. (A) Schematic representation of the NBRE sequence (AAAGGTC) within the $\beta 3$ -integrin promoter region and the mutant sequence (ACATTTCA) used in the avidin-biotin conjugate DNA precipitation assay. Probing was performed using biotinylated or unbiotinylated (competitor) double-stranded $\beta 3$ -integrin wild-type and mutant (MUT) oligonucleotides with whole-cell extracts from Ishikawa cells transfected with Ad-Flag-Nur77. (B) Western blot analysis of Nur77 protein levels in Ishikawa cells transfected with adenoviruses harbouring siNur77 (Ad-siNur77). (C) Ishikawa cells transfected with Ad-siNur77 were treated with oestradiol (E₂; 10⁻⁸ M) and progesterone (P₄; 10⁻⁶ M) for 12 h and then subjected to Western blot analysis of $\beta 3$ -integrin, FAK and pY397-FAK protein levels. (D) Ishikawa cells transfected with Ad-Flag-Nur77 and Ad-Mst1 were subjected to Western blot analysis. (E) Ishikawa cells transfected with Ad-siNur77 and Ad-Mst1 were subjected to Western blot analysis. (F) Ishikawa cells transfected with Ad-Nur77 were treated with 2 μ g/mL cyclo (Arg-Gly-Asp-d-Phe-Lys) (RGDFK) and cyclo (Arg-Gly-Glu-d-Phe-Lys) (RGEFK) and then subjected to BeWo spheroid adhesion assays. ****P* < 0.001 by Tukey's multiple comparisons test.

mid-secretory endometrium from women with RIF (*n* = 14) than that in the normal controls (*n* = 14) (Fig. 7C). Furthermore, we generated a special antibody against phospho-Nur77-Thr366 and found an obvious decrease (by 80%, *P* < 0.001) of pNur77 (T366) protein level in the mid-secretory endometrium from women with RIF (*n* = 14) than that in the normal controls (*n* = 14). The expression of $\beta 3$ -integrin was decreased by 45% (*P* < 0.05) in the mid-secretory endometrium from women with RIF (*n* = 14) than that in the normal controls (*n* = 14), and there was a positive correlation between the protein levels of pNur77 (T366) and $\beta 3$ -integrin (*n* = 28, *r* = 0.46, *P* < 0.05) (Fig. 7D and E). Collectively, these data suggested that the phosphorylation of Nur77 at Thr366 was impaired in the mid-secretory endometrium from women with RIF, indicating the potential importance of Mst1 mediated phosphorylation of Nur77 on the regulation of endometrial receptivity in women.

Discussion

Inadequate endometrial receptivity is responsible for approximately two-thirds of implantation failures.⁴⁷ The underlying mechanism involved in the regulation of $\beta 3$ -integrin by Mst1/Nur77 was explored in this present study, and the potent treatment to promote the embryo-epithelium interaction was proposed. We

found that Mst1 is involved in establishing endometrial receptivity dependent on the kinase activity, and identified Nur77 as a new substrate of Mst1. Mst1 phosphorylates Nur77 at threonine 366 to regulate the transcription of $\beta 3$ -integrin. Importantly, we uncovered that peptide-pThr³⁶⁶ promoted trophoblast-uterine epithelium adhesion *in vitro* and embryo implantation *in vivo*, and endometrial pNur77 (T366) level was aberrantly decreased in women with RIF, indicating the key role of Mst1 mediated phosphorylation of Nur77 on embryo implantation (Fig. 7F).

Nur77 (also known as NR4A1 or TR3) is an immediate early gene that functions as a ligand-independent transcription factor to regulate various biological processes.^{48,49} We previously showed that Nur77 knockout mice exhibited impaired decidualization and a subfertility phenotype, but the molecular mechanism regulating the activity and expression of Nur77 in uteri has not been fully elucidated.²⁶ Multiple phosphorylation sites have been identified in Nur77 regulated by various signalling pathways in different cell systems. The phosphorylation of Ser-351 by Akt decreased the transcriptional activity of Nur77, while phosphorylation of Ser-341 had little or no effect.^{50,51} The phosphorylation of Thr-27 and Thr-143 by p38 α attenuates Nur77 inhibition of NF- κ B activity, leading to enhanced p65 binding capacity to DNA.⁵² Mst1, as a central node of the mammalian Mst-Hippo pathway, is

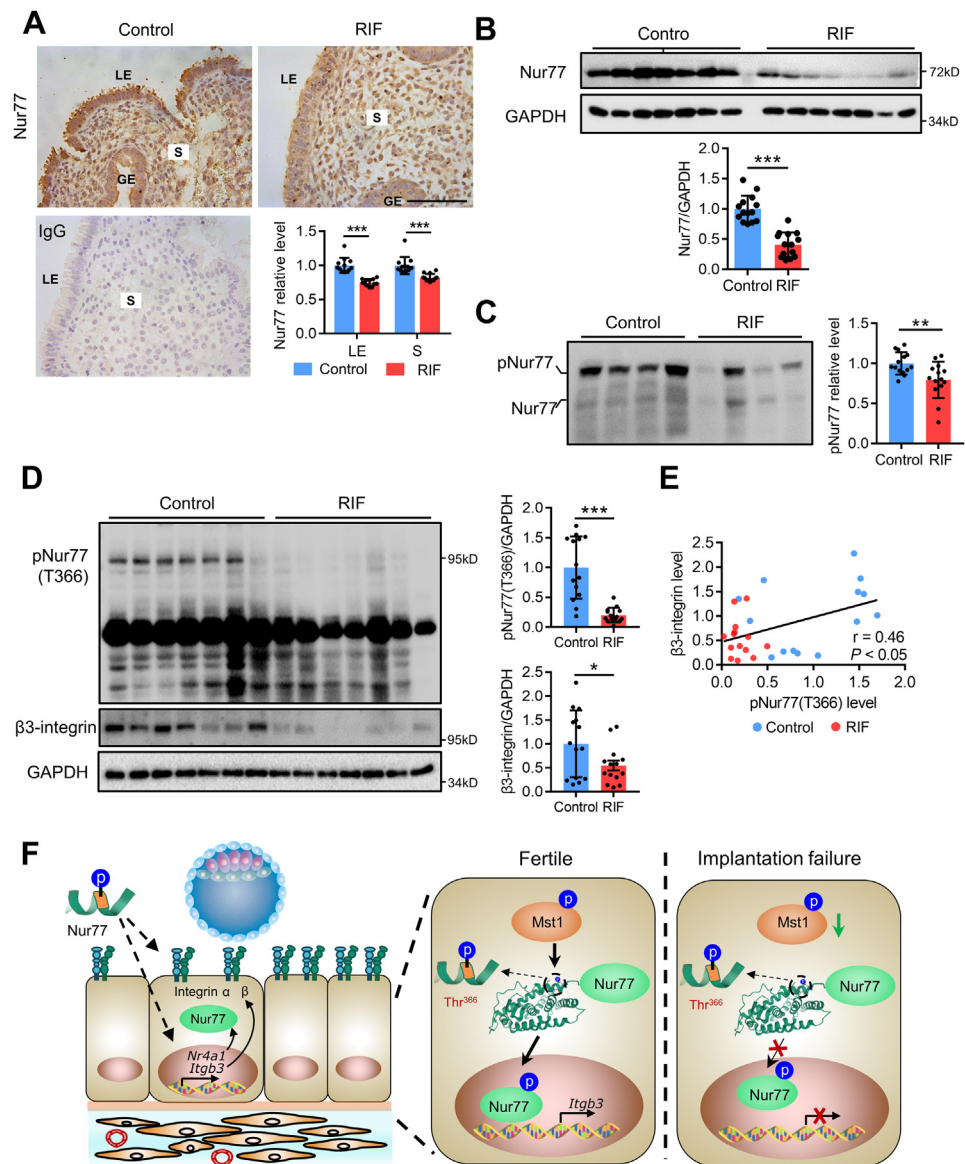


Fig. 7: Impaired phosphorylation of Nur77 in the endometrium of women with unexplained RIF. (A) Immunostaining analysis of mid-secretory endometrial Nur77 protein expression in women with RIF (n = 5) versus normal controls (n = 5). (B) Western blot analysis of Nur77 protein levels in mid-secretory endometrium from infertile women with RIF (n = 14) and normal controls (n = 14). (C) Phos-tag SDS-PAGE analysis of Nur77 and phosphorylated Nur77 protein in mid-secretory endometrium from infertile women with RIF (n = 14) and normal controls (n = 14). (D) Western blot analysis of phospho-Nur77-Thr366 and β 3-integrin protein levels in mid-secretory endometrium from infertile women with RIF (n = 14) and normal controls (n = 14). (E) Pearson correlation analysis of mid-secretory endometrial protein levels of phospho-Nur77-Thr366 and β 3-integrin protein levels ($r = 0.46$, $P < 0.05$) in all samples (n = 28). LE, luminal epithelium; GE, glandular epithelium; S, stroma. Scale bars, 100 μ m * $P < 0.05$, ** $P < 0.01$, *** $P < 0.001$. Student's t test. (F) Graphical abstract. We identified a new post-translational modification of Nur77, phosphorylation of threonine 366 of Nur77 mediated by phosphorylase Mst1, promotes the expression of β 3-integrin. We uncovered a Nur77-derived peptide containing phosphorylated T366 that potently promotes endometrial receptivity by regulating integrin-mediated cell adhesion in mice. Both active Mst1 and phospho-Nur77-Thr366 expression levels were decreased in the endometrium of infertile women with recurrent implantation failure, indicating the similar regulatory mechanism in human.

a multifunctional serine-threonine kinase member of the STE20 family and several substrates have been identified to date, including LATS1/2, FOXO3, and H2B.⁵³ In addition, active Mst1 has been shown to

directly phosphorylate the pro-apoptotic protein BIM, anti-apoptotic proteins BCL-xL and SIRT1 to regulate apoptotic pathways.⁵⁴ In the present study, we found that Mst1, but not kinase activity-deficient Mst1,

promoted Nur77-mediated BeWo spheroid adhesion. Nur77 was recently identified as a target of the Hippo pathway that mediates the pro-apoptotic and anti-tumor effects, whereby YAP promotes Nur77 phosphorylation through AKT.⁵⁵ Herein, *in vitro* kinase assay following with LC-MS/MS assay confirmed that Nur77, as a new substrate of Mst1, was directly phosphorylated at Thr-366, which is a new phosphorylation site that has not been reported previously.

More than 60 peptide drugs have reached the market for the benefit of patients, and several hundred novel therapeutic peptides are in preclinical and clinical development.⁵⁶ Recently, a Nur77-derived peptide with 9 amino acids (NuBCP-9) was shown to induce the apoptosis of cancer cells *in vitro* and in animals by converting Bcl-2 from a protector to a killer of cancer cells, and polymeric nanoparticle encapsulation was utilized to enhance the cell-penetrative ability of NuBCP-9.^{24,25} We speculated that a Nur77-derived peptide may play a role in regulating the process of embryo-epithelium adhesion. To facilitate peptide crossing into the cells, we included the transactivator of transcription (TAT) sequence (GRKKRRQRRRPQ) at the N-terminus of all the peptides.^{57,58} Indeed, a Nur77-derived peptide with 10 amino acids containing phosphorylated T366 increased the rate of adhesion of BeWo spheroids or mouse embryos with Ishikawa cells and the rate of embryo implantation in a delayed implantation mouse model. The functional prediction of the peptide-pThr³⁶⁶-regulated transcriptome via GO analysis and GSEA showed that the “Regulation of cell adhesion” and gene set “Integrin-mediated signalling” pathways were enriched in peptide-pThr³⁶⁶-treated uteri. In particular, β 3-integrin was increased in the epithelial cells of Peptide-pThr³⁶⁶-treated uteri. Dynamic dimer formation is an elaborate means of modulating transcription factor activities, and Nur77 binds the regulatory NBRE as a homodimer or a component of heterodimers formed between subfamily members (NR4A2 and NR4A3).⁵⁹ Previous research has proven that a phosphotyrosyl peptide blocks stat3-mediated DNA-binding activity and gene regulation by regulating stat3 dimerization.⁶⁰ We found that peptide-pThr³⁶⁶ treatment increased the expression of *Nr4a1*, *Nr4a2* and *Nr4a3* (Fig. 5J and Fig. S3), providing a possible mechanism by which peptide-pThr³⁶⁶ promotes integrin-mediated signalling.

The functions of the kinase MST1 rely heavily on its ability to phosphorylate and become phosphorylated themselves on threonine 183.⁶¹ We found that active Mst1 was decreased in the endometrium of women with RIF. β 3-integrin has been proven as an important endometrial receptivity marker, and our data showed that β 3-integrin was a direct downstream target of Nur77. Phosphorylation of Thr-366 mediated by Mst1 enhanced the transcriptional activity of Nur77, which was consistent with the observation that Mst1 promoted the expression of β 3-integrin partly dependent on

Nur77. As expected, the expression level of Nur77 was decreased in the endometrium of women with RIF, while the change of phosphorylated Nur77 was more obvious than that of unphosphorylated Nur77 (Fig. 7C). Furthermore, we generated a special antibody against phospho-Nur77-Thr366 and found an obvious decrease of pNur77 (T366) in the endometrium of women with RIF. It is worth noting that the decline of pNur77 (T366) (by 80%) was more obvious than that of β 3-integrin (by 45%), indicating that pNur77 (T366) has the potential to be a more reliable evaluating marker of endometrial receptivity in the infertile women (Fig. 7D). Overall, we uncovered a Mst1/Nur77/ β 3-integrin signal axis involved in the regulation of endometrial receptivity. Further research is needed to directly ascertain the correlation of phosphorylated Nur77 changes and different pregnancy outcomes. The detailed physical and chemical properties of peptide-pThr366 need to be further identified, and the phosphorylation state-specific antibody against phospho-Nur77-Thr366 could be further purified to improve the antibody testing capacities in endometrial tissues of both human and mice *in situ*. Further exploration of the effect of peptide-pThr366 using more complicated *in vitro* model, such as the ‘assembloid’ model consisting of endometrial gland-like organoids and primary endometrial stromal cells,⁶² would help clarify the key role and regulatory mechanism of peptide-pThr366 during the process of embryo implantation. The human study is limited by its retrospective nature, and a higher sample size or a prospective randomized design could be used in future studies to corroborate the potential effect of peptide-pThr366 on embryo implantation in RIF patients.

Collectively, we identified Nur77 as a new substrate of Mst1, was involved in the regulation of β 3-integrin by phosphorylated at threonine 366, and demonstrated that a Nur77-derived peptide-pThr³⁶⁶ promoted the endometrial receptivity. Aberrantly low endometrial phospho-Nur77 (T366) expression is a promising biomarker for endometrial receptivity. A better understanding of the regulatory network of the Mst1/Nur77/ β 3-integrin signal axis may help to develop related targeted therapy for clinical treatment of recurrent embryo implantation failure in women.

Contributors

G.Y., H.S. and R.J. initiated and supervised the project. R.J., X.C., Y.J., Z.C., N.K., M.Z. and L.Y. performed the experiments, and collected the data; S.K., W.D. and Y.T. contributed to the animal models and animal analysis. G.Y., H.S., J.S., L.D. and H.W. analyzed and discussed the data. R.J. prepared the original draft manuscript, H.S. and G.Y. edited and finalized manuscript. All authors critically read and commented on the manuscript and approved the final version for submission.

Data sharing statement

The authors provide detailed description of methods and original data upon request. RNA-seq data sets generated in this study have been deposited at the Gene Expression Omnibus (GEO) database under accession number GSE198602.

Declaration of interests

The authors declare no competing interests.

Acknowledgements

This work was supported by the National Key Research and Development Program of China (2018YFC1004400 to Guijun Yan), the National Natural Science Foundation of China (82171653 and 30900727 to Guijun Yan, 82030040 to Haixiang Sun, 82271698 to Ruiwei Jiang, and 81971387 to Yue Jiang), the Natural Science Foundation of Jiangsu Province (BK20190051 to Yue Jiang) and National Institutes of Health grants (R01HL103869 to Jianxin Sun).

Appendix A. Supplementary data

Supplementary data related to this article can be found at <https://doi.org/10.1016/j.ebiom.2022.104433>.

References

- Norwitz ER, Schust DJ, Fisher SJ. Implantation and the survival of early pregnancy. *N Engl J Med*. 2001;345:1400–1408.
- Taylor A. ABC of subfertility: extent of the problem. *BMJ*. 2003;327:434–436.
- Macklon NS, Geraedts JPM, Fauser BCJM. Conception to ongoing pregnancy: the 'black box' of early pregnancy loss. *Hum Reprod Update*. 2002;8:333–343.
- Luke B, Brown MB, Wantman E, et al. Cumulative birth rates with linked assisted reproductive technology cycles. *N Engl J Med*. 2012;366:2483–2491.
- Coughlan C, Ledger W, Wang Q, et al. Recurrent implantation failure: definition and management. *Reprod Biomed Online*. 2014;28:14–38.
- Kliman HJ, Frankfurter D. Clinical approach to recurrent implantation failure: evidence-based evaluation of the endometrium. *Fertil Steril*. 2019;111:618–628.
- Nikas G. Endometrial receptivity: changes in cell-surface morphology. *Semin Reprod Med*. 2000;18:229–235.
- Zhang S, Lin H, Kong S, et al. Physiological and molecular determinants of embryo implantation. *Mol Aspects Med*. 2014;34:939–980.
- Dey SK, Lim H, Das SK, et al. Molecular cues to implantation. *Endocr Rev*. 2004;25:341–373.
- Aplin JD, Kimber SJ. Trophoblast-uterine interactions at implantation. *Reprod Biol Endocrinol*. 2004;2:48.
- Lessey BA, Castelbaum AJ. Integrins and implantation in the human. *Rev Endocr Metab Disord*. 2002;3:107–117.
- Lessey BA, Damjanovich L, Coutifaris C, Castelbaum A, Albeida SM, Buck CA. Integrin adhesion molecules in the human endometrium. Correlation with the normal and abnormal menstrual cycle. *J Clin Invest*. 1992;90:188–195.
- Lessey BA, Castelbaum AJ, Sawin SW, Sun J. Integrins as markers of uterine receptivity in women with primary unexplained infertility. *Fertil Steril*. 1995;63:535–542.
- Yan Q, Huang C, Jiang Y, et al. Calpain7 impairs embryo implantation by downregulating $\beta 3$ -integrin expression via degradation of HOXA10. *Cell Death Dis*. 2018;9:41419.
- Illera MJ, Cullinan E, Gui Y, Yuan L, Beyler SA, Lessey BA. Blockade of the $\alpha(v)\beta(3)$ integrin adversely affects implantation in the mouse. *Biol Reprod*. 2000;62:1285–1290.
- Coughlan C. What to do when good-quality embryos repeatedly fail to implant. *Best Pract Res Clin Obstet Gynaecol*. 2018;53:48–59.
- Craciunas L, Tsampras N, Raine-Fenning N, Coomarasamy A. Intrauterine administration of human chorionic gonadotropin (hCG) for subfertile women undergoing assisted reproduction. *Cochrane Database Syst Rev*. 2018;10:CD011537.
- Kamath MS, Kirubakaran R, Sunkara SK. Granulocyte-colony stimulating factor administration for subfertile women undergoing assisted reproduction. *Cochrane Database Syst Rev*. 2020;1:CD013226.
- Makrigiannakis A, Makrygiannakis F, Vrekoussis T. Approaches to improve endometrial receptivity in case of repeated implantation failures. *Front Cell Dev Biol*. 2021;9:613277.
- Li S, Zou Q, Xing R, Govindaraju T, Fakhruллин R, Yan X. Peptide-modulated self-assembly as a versatile strategy for tumor supramolecular nanotherapeutics. *Theranostics*. 2019;9:3249–3261.
- Rosario GX, Modi DN, Sachdeva G, Manjramkar DD, Puri CP. Morphological events in the primate endometrium in the presence of a preimplantation embryo, detected by the serum preimplantation factor bioassay. *Humanit Rep*. 2005;20:61–71.
- Barnea ER, Almogi-Hazan O, Or R, et al. Immune regulatory and neuroprotective properties of preimplantation factor: from newborn to adult. *Pharmacol Ther*. 2015;156:10–25.
- Barnea ER, Kirk D, Paidas MJ. PreImplantation Factor (PIF) promoting role in embryo implantation: increases endometrial Integrin- $\alpha 2\beta 3$, amphiregulin and epiregulin while reducing betacellulin expression via MAPK in decidua. *Reprod Biol Endocrinol*. 2012;10:50.
- Kolluri SK, Zhu X, Zhou X, et al. A short Nur77-derived peptide converts Bcl-2 from a protector to a killer. *Cancer Cell*. 2008;14:285–298.
- Kumar M, Gupta D, Singh G, et al. Novel polymeric nanoparticles for intracellular delivery of peptide cargos: antitumor efficacy of the BCL-2 conversion peptide NuBCP-9. *Cancer Res*. 2014;74:3271–3281.
- Jiang Y, Jiang R, Cheng X, et al. Decreased expression of NR4A nuclear receptors in adenomyosis impairs endometrial decidualization. *Mol Hum Reprod*. 2016;22:655–668.
- Lucas ES, Vrljicak P, Muter J, et al. Recurrent pregnancy loss is associated with a pro-senescent decidual response during the peri-implantation window. *Commun Biol*. 2020;3:37.
- Polanski LT, Baumgarten MN, Quenby S, Brosens J, Campbell BK, Raine-Fenning NJ. What exactly do we mean by 'recurrent implantation failure'? A systematic review and opinion. *Reprod Biomed Online*. 2014;28:409–423.
- Ma W-g, Song H, Das SK, Paria BC, Dey SK. Estrogen is a critical determinant that specifies the duration of the window of uterine receptivity for implantation. *Proc Natl Acad Sci U S A*. 2003;100:2963–2968.
- Sheng X, Liu C, Yan G, et al. The mitochondrial protease LONP1 maintains oocyte development and survival by suppressing nuclear translocation of AIFM1 in mammals. *eBioMedicine*. 2022;75:103790.
- Ren A, Yan G, You B, Sun J. Down-regulation of mammalian sterile 20-like kinase 1 by heat shock protein 70 mediates cisplatin resistance in prostate cancer cells. *Cancer Res*. 2008;68:2266–2274.
- You B, Jiang YY, Chen S, Yan G, Sun J. The orphan nuclear receptor Nur77 suppresses endothelial cell activation through induction of I κ B α expression. *Circ Res*. 2009;104:742–749.
- Zhang H, Zhu X, Chen J, et al. Krüppel-like factor 12 is a novel negative regulator of forkhead box O1 expression: a potential role in impaired decidualization. *Reprod Biol Endocrinol*. 2015;13:80.
- Wen W, Zhu F, Zhang J, et al. MST1 promotes apoptosis through phosphorylation of histone H2AX. *J Biol Chem*. 2010;285:39108–39116.
- Graves JD, Gotoh Y, Draves KE, et al. Caspase-mediated activation and induction of apoptosis by the mammalian Ste20-like kinase Mst1. *EMBO J*. 1998;17:2224–2234.
- Kinoshita E, Kinoshita-Kikuta E, Koike T. Separation and detection of large phosphoproteins using phos-tag sds-page. *Nat Protoc*. 2009;4:1513–1521.
- Bekešová S, Komis G, Křenek P, et al. Monitoring protein phosphorylation by acrylamide pendant Phos-TagTM in various plants. *Front Plant Sci*. 2015;6:336.
- Liu J, Jiang S, Zhao Y, et al. Geranylgeranyl diphosphate synthase (GGPPS) regulates NAFLD/fibrosis progression by determining hepatic glucose/fatty acid preference under high-fat-diet conditions. *J Pathol*. 2018;246:277–288.
- Jiang R, Ding L, Zhou J, et al. Enhanced HOXA10 sumoylation inhibits embryo implantation in women with recurrent implantation failure. *Cell Death Discov*. 2017;3:17057.
- Kang YJ, Forbes K, Carver J, Aplin JD. The role of the osteopontin-integrin $\alpha v\beta 3$ interaction at implantation: functional analysis using three different in vitro models. *Humanit Rep*. 2014;29:739–749.
- Zhou Y, Zhou B, Pache L, et al. Metascape provides a biologist-oriented resource for the analysis of systems-level datasets. *Nat Commun*. 2019;10:1523.
- Charan J, Kantharia N. How to calculate sample size in animal studies? *J Pharmacol Pharmacother*. 2013;4:303–306.
- Somkuti SG, Yuan L, Fritz MA, Lessey BA. Epidermal growth factor and sex steroids dynamically regulate a marker of endometrial receptivity in ishikawa cells. *J Clin Endocrinol Metab*. 1997;82:2192–2197.

- 44 Wang H, Zhang S, Lin H, et al. Physiological and molecular determinants of embryo implantation. *Mol Aspects Med.* 2013;34:939–980.
- 45 Lim HJ, Wang H. Uterine disorders and pregnancy complications: insights from mouse models. *J Clin Invest.* 2010;120:1004–1015.
- 46 Chen JR, Cheng JG, Shatzer T, Sewell L, Hernandez L, Stewart CL. Leukemia inhibitory factor can substitute for nidatory estrogen and is essential to inducing a receptive uterus for implantation but is not essential for subsequent embryogenesis. *Endocrinology.* 2000;141:4365–4372.
- 47 Achache H, Revel A. Endometrial receptivity markers, the journey to successful embryo implantation. *Hum Reprod Update.* 2006;12:731–746.
- 48 Winoto A, Littman DR. Nuclear hormone receptors in T lymphocytes. *Cell.* 2002;109(Suppl):S57–S66.
- 49 Wu L, Chen L. Characteristics of Nur77 and its ligands as potential anticancer compounds. *Mol Med Rep.* 2018;18:4793–4801.
- 50 Pekarsky Y, Hallas C, Palamarchuk A, et al. Akt phosphorylates and regulates the orphan nuclear receptor Nur77. *Proc Natl Acad Sci U S A.* 2001;98:3690–3694.
- 51 Hirata Y, Kiuchi K, Chen HC, Milbrandt J, Guroff G. The phosphorylation and DNA binding of the DNA-binding domain of the orphan nuclear receptor NGFI-B. *J Biol Chem.* 1993;268:24808–24812.
- 52 Li L, Liu Y, Chen HZ, et al. Impeding the interaction between Nur77 and p38 reduces LPS-induced inflammation. *Nat Chem Biol.* 2015;11:339–346.
- 53 Rawat SJ, Chernoff J. Regulation of mammalian Ste20 (Mst) kinases. *Trends Biochem Sci.* 2015;40:149–156.
- 54 Del Re DP, Matsuda T, Zhai P, et al. Mst1 promotes cardiac myocyte apoptosis through phosphorylation and inhibition of Bcl-xL. *Mol Cell.* 2014;54:639–650.
- 55 He L, Yuan L, Yu W, et al. A regulation loop between YAP and NR4A1 balances cell proliferation and apoptosis. *Cell Rep.* 2020;33:108284.
- 56 Fosgerau K, Hoffmann T. Peptide therapeutics: current status and future directions. *Drug Discov Today.* 2015;20:122–128.
- 57 Gupta B, Levchenko TS, Torchilin VP. Intracellular delivery of large molecules and small particles by cell-penetrating proteins and peptides. *Adv Drug Deliv Rev.* 2005;57:637–651.
- 58 Otto M, Bucher C, Liu W, et al. 12(S)-HETE mediates diabetes-induced endothelial dysfunction by activating intracellular endothelial cell TRPV1. *J Clin Invest.* 2020;130:4999–5010.
- 59 Maira M, Martens C, Batsché É, Gauthier Y, Drouin J. Dimer-specific potentiation of NGFI-B (Nur77) transcriptional activity by the protein kinase A pathway and AF-1-dependent coactivator recruitment. *Mol Cell Biol.* 2003;23:763–776.
- 60 Turkson J, Kim JS, Zhang S, et al. Novel peptidomimetic inhibitors of signal transducer and activator of transcription 3 dimerization and biological activity. *Mol Cancer Ther.* 2004;3:261–269.
- 61 Radu M, Chernoff J. The DeMSTification of mammalian Ste20 kinases. *Curr Biol.* 2009;19:R421–R425.
- 62 Rawlings TM, Makwana K, Taylor DM, et al. Modelling the impact of decidual senescence on embryo implantation in human endometrial assembloids. *Elife.* 2021;10:e69603.